

Transcriptomic and genomic analysis highlights the basis of ZYMV tolerance in zucchini

Ciro Amoroso

University of Naples Federico II

Giuseppe Andolfo

University of Naples Federico II

Claudio Capuozzo

University of Naples Federico II

Antimo Di Donato

University of Naples Federico II

Cecilia Martinez

University of Almería

Laura Tomassoli

Agricultural Research Council

Maria Ercolano (✉ ercolano@unina.it)

University of Naples Federico II

Research Article

Keywords: Cucurbita pepo, RNA-seq, Transcriptome, Molecular markers, Plant recovery, Plant Virus

Posted Date: January 4th, 2021

DOI: <https://doi.org/10.21203/rs.3.rs-134049/v1>

License:   This work is licensed under a Creative Commons Attribution 4.0 International License.

[Read Full License](#)

1 **Transcriptomic and genomic analysis highlights the basis**
2 **of ZYMV tolerance in zucchini**

3 **Amoroso CG¹, Andolfo G¹, Capuozzo C¹, Di Donato A¹, Martinez C², Tomassoli L³, Ercolano MR***

4 ¹ Department of Agricultural Science – University of Naples “Federico II” – Portici (NA)

5 ² Department of Biology and Geology, Research Centers CIAIMBITAL and Ceia3, University of Almería, 04120
6 Almería, Spain

7 ³ Consiglio per la Ricerca in Agricoltura e l'Analisi dell'Economia Agraria, Research Centre of Plant Control and
8 Certification, Rome, Italy

9

10

11

12

13

14

15

16

17

18

19

20

21

22 * Corresponding author: Maria Raffaella Ercolano, Department of Agricultural Sciences, University of Naples Federico

23 II. Via Università 100, 80055 Portici (Naples), Italy. ercolano@unina.it

24

25 **Abstract**

26 **Background:** *Cucurbita pepo* is high susceptible to Zucchini yellow mosaic virus (ZYMV) and the resistance
27 found in several wild species does not provide complete or broad-spectrum resistance. In this study, a source
28 of tolerance introgressed in *C. pepo* (381e) from *C. moschata*, in True French (TF) background, was investigated
29 12 days post inoculation (DPI) at transcriptomic and genomic levels.

30 **Results:** A comparative RNA-seq experiment on TF (susceptible to ZYMV) and 381e (tolerant to ZYMV),
31 allowed to evaluate 33,000 expressed transcripts and to identify 146 differentially expressed genes (DEGs) in
32 381e, mainly involved in photosynthesis, transcription, cytoskeleton organization and callose synthesis. By
33 contrast, the susceptible line True French triggered oxidative processes related to response to biotic stimulus,
34 and key regulators of plant virus intercellular movement. Moreover, the genome mapping of transcripts
35 allowed the identification of two chromosome regions rich in SNPs (Single Nucleotide Polymorphisms),
36 putatively introgressed from *C. moschata*, containing genes exclusively expressed in 381e.

37 **Conclusion:** The transcriptome reprogramming of 381e ZYMV challenged revealed a globally restoring of
38 cellular activities and a reduced virus movement and replication. Furthermore, genes putatively involved in
39 ZYMV tolerance were detected in *C. moschata* introgressed genomic regions. Our work provides new insight
40 into the plant virus recovery process and a better understanding of the molecular basis of 381e tolerance.

41 **Keywords:** *Cucurbita pepo*, RNA-seq, Transcriptome, Molecular markers, Plant recovery, Plant Virus

42

43

44 1. Background

45 *Cucurbita pepo* is a high polymorphic species including economically important crops grown worldwide.
46 This species is high susceptible to Zucchini yellow mosaic virus (ZYMV), a quickly spread potyvirus aphid
47 transmitted, leading to leaf yellowing and deformations, stunting and fruit defects [1-3]. Till now, no sources
48 of resistance to ZYMV have been found in this species though in many areas it results one of the most serious
49 threat limiting crop production.

50 A wide range of ZYMV resistant genetic resources was found in other *Cucurbita* species [4,5]. Several *C.*
51 *moschata* accessions carrying resistance genes to ZYMV were identified: Nigerian local carrying “*zym0*” and
52 “*zym4*” resistance gene [6]; Menina and Bolina possessing a resistance gene named “*Zym1*” [7]; Soler accession
53 containing the recessive gene “*zym6*” [8] and four genes that confer resistance to ZYMV were also identified
54 in “*OttoF1*” variety [9].

55 The genetic inheritance of resistance/tolerance derived from Menina in the *C. pepo* background showed
56 that *Zym-1* gene could interact with minor genes able to modulate the defense response [6,10]. Recently,
57 Capuozzo et al., [11] investigated *Zym-1* segregation in different *C. pepo* populations highlighting segregation
58 anomaly left over from the original interspecific cross between *C. pepo* and *C. moschata*. Genetic analysis for
59 tolerance to ZYMV, at both the phenotypic and genotypic level, indicated clearly that a major gene, *Zym-1* is
60 essential for a tolerance expression in 381e genotype background but putative additional genes with additive
61 and/or epistatic effects may mitigate or delay the symptoms. Pachner et al., reported that the combined
62 deployment of 7 genes in *C. pepo*, would be required for maximal expression of ZYMV tolerance [12]. The
63 involvement of putative modifying minor genes made difficult the understanding of genetic control and the
64 subsequently the transfer of ZYMV tolerance in breeding lines. In addition, the tolerant cultivar 381e during
65 ZYMV challenging showed a systemic symptomatic infection 4 days after inoculation (DPI) and a plant
66 recovery, characterized by the emergence of newly developing leaves about 12 days after inoculation that can
67 hamper genetic analysis [10].

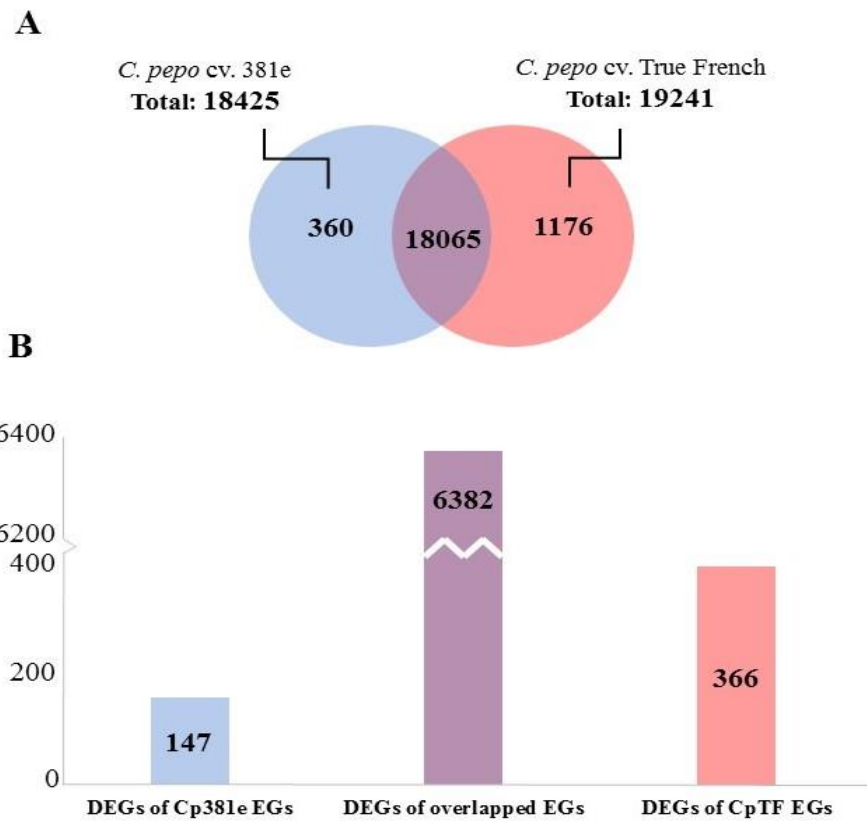
68 Cucurbit genomic analysis and comparative gene expression analysis resulted very useful for overcoming
69 the difficulties related to introgression of desirable traits and for dissecting the molecular basis of host
70 tolerance [13-15]. A reference zucchini genome version 4.1 (BGV004370) was recently provided and several *C.*
71 *pepo* next-generation sequencing technologies as RNA-sequencing (RNA-seq) have been explored [16-19]. To
72 date, RNA-seq technology provides new opportunities for mapping and quantifying transcripts, creating new
73 opportunities for comprehension of pathways activated during plant-pathogen interaction and of genomic
74 regions underlying the genes involved.

75 The main goal of this work was to investigate the mechanism of ZYMV tolerance by the means of genome-
76 wide transcriptional analysis of the susceptible TF cultivar and of a tolerant derived line 381e. The
77 remodulation of genome expression in virus-infected plants were assessed at 12 DPI to better highlight key
78 genes activated in the plant recovering process in the tolerant accession. In addition, to facilitate the
79 identification the candidate genes involved in ZYMV tolerance in *C. moschata* introgressed regions a genomic
80 scanning was performed.

81 **2. Results**

82 2.1 *C. pepo* transcriptional profile upon ZYMV inoculation

83 The transcriptomic reprogramming of two zucchini isogenic cultivars (TF and derived ZYMV tolerant
84 line 381e) inoculated with (ZYMV), were evaluated by analysing 33,388 genes expressed at 12 DPI (days post
85 inoculation). In TF-ZYMV interaction, transcriptome variation resulted in 19,241 total expressed genes. As for
86 the cultivar 381e, 18,425 total transcripts were observed upon inoculation with ZYMV (Fig 1A). Private
87 expressed genes (360) in 381e were more than three times less than TF (1,176). Out of a total of 18,065
88 overlapping transcripts 6,382 were differentially expressed in the both cultivars; 147 were differentially
89 expressed in 381e and 366 in TF (Fig. 1B). Among the 3,681 upregulated genes (FDR-adjusted p-value, 0.01),
90 147 resulted exclusively up regulated in 381e, suggesting that they play an important role in recovery during
91 virus infection. The two transcriptomes virus challenged were further investigated to understand in which
92 biological processes were involved the differentially expressed genes (DEGs) identified.



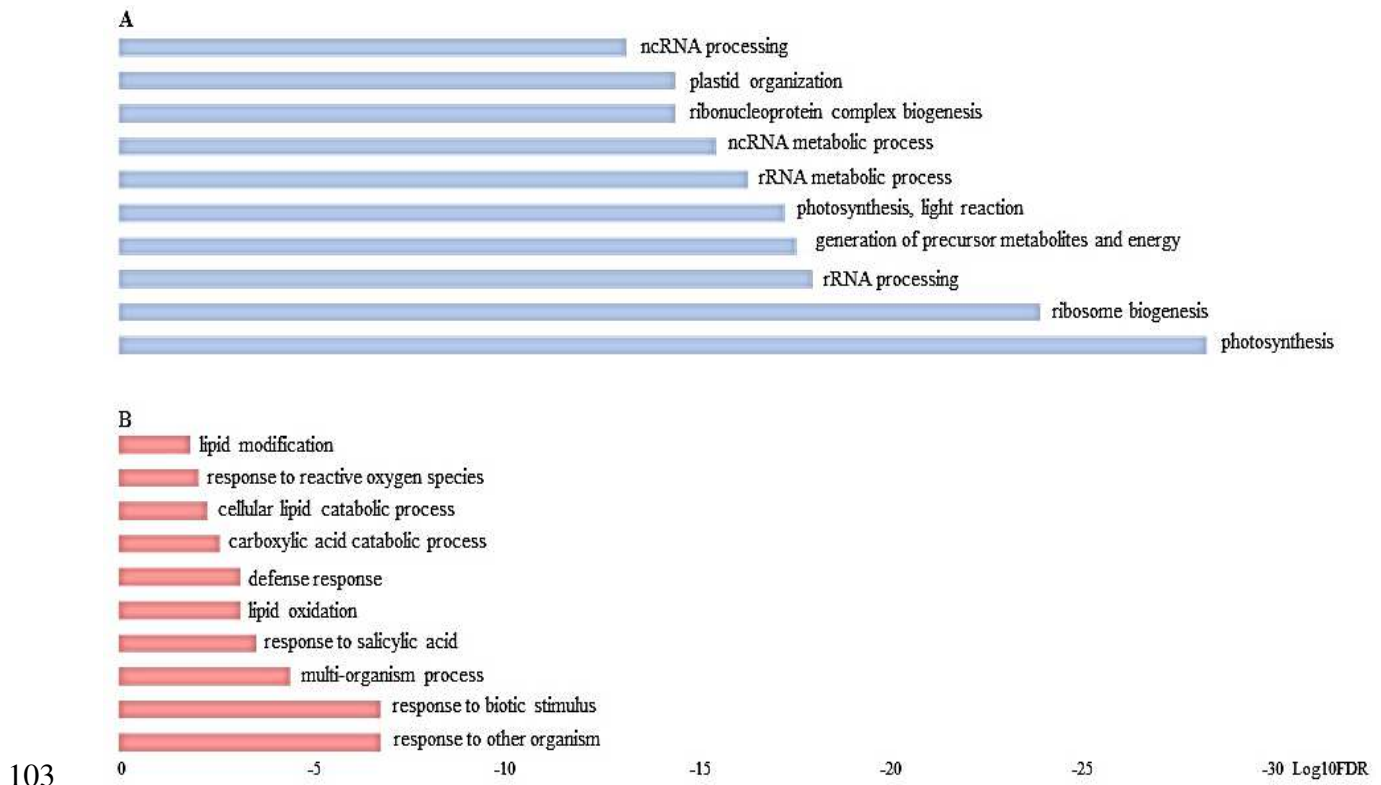
93

94 **Figure 1.** Transcriptional Profile. A) Total Expressed Genes in *C. pepo* 381e (blue), TF (orange), and overlapped
 95 genes (violet). B) Differentially Expressed Genes for each area of Venn diagram.

96 2.2 Overview of cellular processes activated in the tolerant and susceptible line

97

98 According to phenotypic recovery observed at 12DPI, the tolerant cultivar 381e showed the restoring of
 99 main cellular activities (transcription, protein translation, photosynthesis, metabolites biosynthesis and
 100 general cellular organization) belonging to 139 GO term enriched categories. By the contrast, the susceptible
 101 cultivar TF showed 32 overrepresented GO terms, principally receptors involved in response to biotic stress,
 102 enzymes for ROS production, peptide degradation and lipid oxidation (Figure 2).



104 **Figure 2.** Top ten of non-redundant significantly enriched GO terms in biological process category. A)
 105 Upregulated genes in 381e and B) Upregulated genes in True French. The categories size is related to LOG₁₀
 106 FDR of enriched GOs.

107

108 The plant vegetative restoring in 381e is promoted by photosynthetic activity through the up regulation
 109 of genes involved in the formation of the photosystems (i.e. Cup000001g001195.1), in the electron transport
 110 chain and in membrane transporters. In addition, genes directly involved in mitochondrial activity, in the
 111 glycolysis process (PEP, Acetyl-CoA, GAPDH, Hexokinaes) in phospholipids synthesis (CDP-alcohol
 112 phosphatidyltransferase) and in shikimic acid network synthesis, resulted strongly up regulated in 381e,
 113 suggesting an overall enhanced photo-respiratory activity. A strong up regulation of genes involved in
 114 helicase activity in 381e, including DEAD-box ATP-dependent RNA helicases, DNA replication licensing
 115 factor such as the exclusively expressed Cup000013g012986.1 and two "DNA-binding protein"
 116 (Cup000085g037850.1 Cup000022g020052.1) was observed. Moreover, several HSPs proteins were found
 117 differentially regulated in both lines. In particular, 381e activated Cup001195g045603.1 an Heat Shock protein-

118 (HSP 90-5) that could be involved in newly synthesized proteins transporting, from ribosomes to chloroplasts
119 and an HSP-70 (Cup000010g010288.1), involved in proteins trafficking through the chloroplast membrane to
120 stroma in cooperation with 14-3-3 protein (Cup000060g034360.1), that resulted overexpressed [20].
121 Furthermore, 7 aquaporin membrane transporters (i.e. Cup000679g045055.1) resulted strongly upregulated in
122 381e (LogFC >1).

123 By contrast, TF showed an high activation of genes involved in the chloroplast architecture (i.e.
124 Cup000003g002638.1), oxygen scavenging such as 2 L-ascorbate peroxidase for H₂O₂ formation
125 (Cup000004g003828.1; Cup000052g032798.1), catalase and superoxide dismutase (i.e. Cup000032g025333.1)
126 and a protein ridA (Cup000182g042991.1) to prevent damage from BCAT3 (Branched-chain-amino-acid
127 aminotransferase 3) that is produced in response to stress. It is interesting to note the up regulation of several
128 cytochromes type p450, associated with the endoplasmic reticulum, involved in metabolism of chemical
129 compounds extraneous to the organism. Among them, a cytochrome CYP82C2 (Cup000001g001147.1), directly
130 involved in the jasmonic acid network synthesis was high expressed, suggesting that the plant defence system
131 is still alerted [21]. In addition, two synaptotagmin and SNAP receptors (Cup000004g004336.1;
132 Cup000029g023659.1; Cup000011g011417.1) resulted up regulated and exclusively expressed in TF.

133 In our study 29 serine/threonine protein kinases, of which 22 were localized on the plasma membrane,
134 resulted up regulated in 381e while 42 in TF. In addition, TF differentially expressed several genes involved
135 in the cell wall degradation (ie. pectin-esterases, beta-glucosidases and Xyloglucan endo-transglycosylases),
136 indicating the collapse of the primaries structure of the plants. On the other hand, it is interesting to note that
137 genes involved in cytoskeleton organisation (Cup000006g006297.1; Cup000010g010383.1;
138 Cup000021g019231.1) resulted exclusively up regulated in 381e as well as a gene involved in
139 glycosaminoglycan biosynthesis (Cup000019g017783.1), two Rab GTP-ases (Cup000067g035924.1;
140 Cup000038g027690.1) and a gene having an important role in the callose synthesis (Cup000021g019191.1).

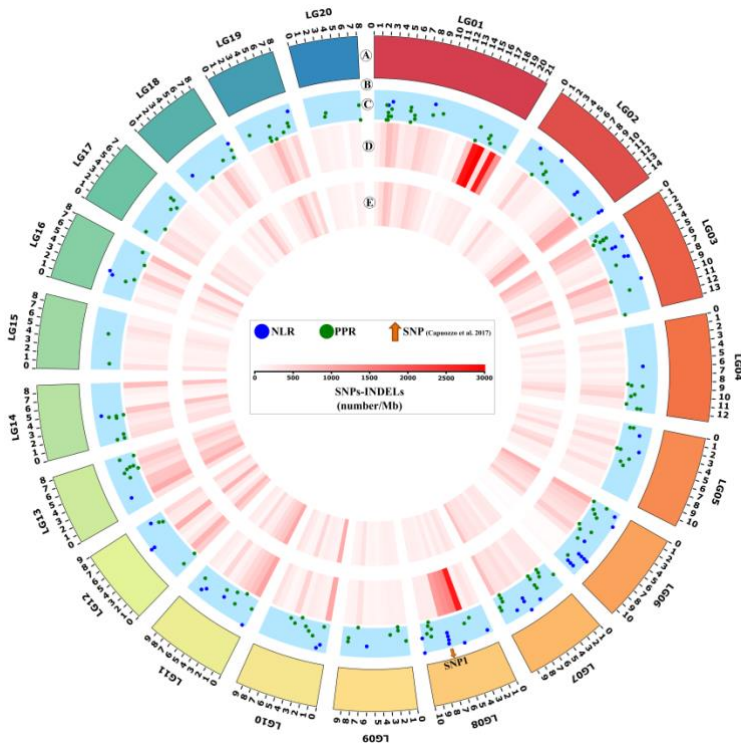
141

142 2.3 Genomic localization of transcript variants

143

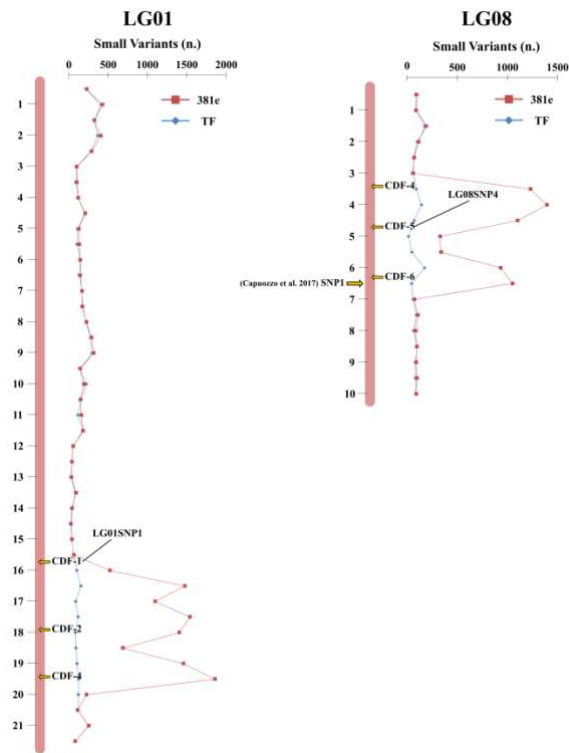
144 In order to identify the putative genomic regions introgressed into *C. pepo* from *C. moschata* cv. Menina,
145 we performed a variant calling with respect of small variants (SNVs: SNPs single nucleotide polymorphisms;
146 INDELs insertions and deletions) for the two near isogenic lines (TF and 381e).

147 A total of 150,605 high-quality small variants were mapped to the *C. pepo* BGV004370 reference genome
148 (Figure 3) [16]. The number of small variants in 381e and TF common expressed genes were normalised respect
149 to the LG (Linkage Group) length (Figure 3). In 381e, on average 8 short variants were mapped for expressed
150 locus on 1 and 8 LGs, while in TF 2 variants per transcript were found on such LGs (Additional Table 2).
151 About 30% of small variants identified in '381e' were mapped on two linkage groups, whilst in TF the
152 percentage of variants on the same LGs was close to 13% (Additional Tables 1 and 2 and Figure 3). Close-up
153 view on 1 and 8 LGs of two *C. pepo* cultivars underlined two genomic regions potentially introgressed from
154 resistant *C. moschata* cv. Menina (Figure 4). Indeed, the 20% (16,891) of small variants identified in 381e were
155 concentrated in two short regions of 1 and 8 LGs, while in TF less than 3% (1,410) were mapped in the same
156 areas. Over 65% (10,321) of small variants identified on LG01 were located on a genomic region of about 4 Mb
157 in 381e. The second putative introgression region of 3,5 Mb showed 82% (6,570) of total variants mapped on
158 LG08 in 381e. Interestingly, Capuozzo et al., have mapped on the same region of LG08 the marker (SNP1)
159 associated to ZYMV tolerance in '381e' (Figure 4 and Additional Table 2) [11].



160

161 **Figure 3.** Circos plot integrating the genomic positions of ZYMV-related markers, pathogen recognition genes
 162 and small variants (SNP: single nucleotide polymorphisms and InDel: insertion and deletion). Inset legend
 163 providing information represented by each data ring. Track A denotes the 20 pseudo-chromosomes (LG:
 164 linkage group) of *Cucurbita pepo*. The length of each circle segment represents the size of pseudo-chromosomes
 165 expressed in megabases (Mb). B) The marker associated to ZYMV tolerance identified by Capuozzo et al. [11]
 166 is indicated by orange arrow. C) Genomic positions of nucleotide binding like proteins (NLR; blue spots) and
 167 receptor like proteins and receptor like kinase (PPR; green spots), annotated by Andolfo et al. [19] , are shown
 168 as scatterplots. Heatmaps for the density levels (number/Mb) of small variants identified in (D) *C. pepo* 381e
 169 and (E) *C. pepo* TF cultivars.



170

171 **Figure 4.** High resolution map integrating genomic and genetic marker information. The distribution of small
 172 variants along 1 and 8 pseudochromosomes was reported (381e in red and TF in blue). The genomic position
 173 of six coding DNA fragments (CDFs) and two CAPS markers (LG01SNP1 and LG08SNP4) was indicated.

174 2.4 Variants validation and marker-phenotype correlation

175 To confirm the DNA variants identified on putative introgression regions located on LG01 and LG08 a
 176 molecular validation was performed. A total of six coding DNA fragments (CDFs) located on two genomic
 177 regions inherited from *C. moschata* were sequenced and analysed (Figure 4). The about 70 SNP calling-related
 178 variants annotated into the 6 CDFs were confirmed from Sanger sequencing (Additional Table 3). Two high
 179 confidence variants (LG08SNP4 and LG01SNP1) were converted in CAPS markers (Additional Table 3;
 180 Additional Figure 1) to conduct a marker-phenotype correlation analysis on a subset of the F2 segregating
 181 population (381e x TF) phenotyped by Capuozzo et al. [11]. LG08SNP4 was physically close (~ 2 Mb) to the
 182 previously mapped “SNP1” and exhibited a very high correlation coefficient (Pearson test p-value << 0,01;
 183 r=0,991) with phenotypic data [11]. In particular, marker correlation with ZYMV-resistance/susceptibility traits

184 was in accordance for 73 genotypes out of 82 genotypes analysed. A good correlation coefficient with
185 phenotypic results was displayed also by LG01SNP1 ($r=0,827$; Pearson test p -value $< 0,05$). In addition, an
186 interesting correlation trend ($r=0,895$; Pearson test p -value $< 0,05$) was identified between the LG01SNP1
187 marker located on chromosome 1 and LG08SNP4 marker located on chromosome 8.

188 3. Discussion

189 From its first report in the late 1970s, ZYMV continued its worldwide expansion, causing cucurbits
190 important yield losses. In this work, we explored the molecular basis of ZYMV tolerance identified in *Cucurbita*
191 *moschata* cv Menina analysing the *C. pepo* derived tolerant cv 381e and its susceptible counterpart TF, through
192 an integrated transcriptomic and genomic experiment. Though *C. moschata* is sparingly cross-fertile with *C.*
193 *pepo*, the gene expression may be hampered in new genomic background [6]. In addition, approximately at 12
194 days after ZYMV inoculation, 381e plants showed a vegetative recovery [10], while damaged TF plants
195 displayed yellowing of foliage, internodes shortening and leaf deformations. In our experiment, an opposite
196 response to infection at 12 DPI in terms of expressed and differentially regulated genes between the two
197 analyzed contrasting genotypes was clearly observed. ZYMV virus usually takes about 9 days to infect the
198 plant systemically through the phloem [22]; and the early systemic infection of 381e, about 4 DPI, was able to
199 prompt a plant recovery. At initial, stage of infection, the plant moderates its immune response and the general
200 fitness, triggering to a decreasing in symptoms of viral infection [23]. The 381e physiological perturbations
201 imposed various constraints to face virus and limiting the synthesis of host proteins essential for replication
202 and movement. Tolerant plants react to virus infection through changes in physiological and developmental
203 processes to limit the synthesis of factors required for virus multiplication [24-26]. We found several DEAD-
204 box RNA helicases and DNA helicase such as Cup000013g012986.1 up regulated in 381e. DEAD-box RNA
205 helicases can function as viral RNA sensors or as effectors by blocking RNA virus replication. RH30 (Dead-
206 box helicase) in tomato was required to restrict bushy stunt virus (TBSV) replication [27]. Moreover, RNA and
207 DNA helicases can also exert a positive role in stress tolerance [28]. A general gene down regulation could be
208 useful to impede virus movement and replication, leading to a less virus titer and promoting a consequent

209 plant recovery [23]. By contrast, the up regulation of factors correlated with transcription process observed in
210 TF plants may facilitate the use the host nuclear factors for ZYMV replication [29].

211 The response to viral infection in 381e required a global host transcriptome reprogramming to avoid the
212 development of most severe symptoms. Indeed, an up-regulation of genes involved in energy production and
213 cell repairing at 12 dpi was observed. In our experiment, the tolerant cultivar 381e showed an increased
214 photosynthetic and photo-respiratory activity to promote the recovery and symptom alleviation. The partially
215 resistant cultivar Jaguar, 15 day after ZYMV inoculation, showed a strong up regulation several proteins
216 involved in photosystems activities [30]. Interestingly, we found a high up regulated gene coding for an
217 HSP90.5 (Cup001195g045603.1) with a LogFC of 4.6 privately expressed in 381e. A properly control
218 of HSP90.5 expression is required for plant growth and development and is especially essential for the
219 chloroplast thylakoid formation and the regulation of the receptor proteins involved in plant immunity [31-
220 33]. In addition, the overexpressed HSP70 (Cup000010g010288.1) cooperate with the overexpressed 14-3-3
221 chaperone (Cup000060g034360.1) to keep the chloroplast or mitochondrial precursor proteins in an unfolded
222 state, acting as a motor for transporting the precursor proteins interacting with the plasmodesmata in
223 translocation pathway [34,35]. By contrast, the TF photosynthetic system was affected by the down regulation
224 of the genes involved in chloroplasts and thylakoids formation.

225 Symptom recovery is generally accompanied by activation of pathogen receptor genes and other defence-
226 related genes during the plant-pathogen interaction [23,36,37]. In particular, we found a resistance protein
227 (CNL) annotated by Andolfo et al., [19] and located on linkage group 8 scaffold 3 (Cup000003g003423.1) up
228 regulated and privately expressed (LogFC 1.51) in 381e [19,38,39]. It is interesting to note that in such transcript
229 we found a variant that could lead to functional modification. In our study, numerous genes codifying for
230 serine/threonine kinases proteins differentially expressed in both lines were also found. These proteins play a
231 central role in signalling during the pathogen's recognition and the subsequent activation of plant defence
232 mechanisms. A serine/threonine kinases belonging to RIO protein family, down regulated and privately
233 expressed in TF (Cup000024g021133.1), were located on linkage group one (scaffold 24) corresponding to one
234 of regions putative introgressed from Menina in 381e. These proteins are generally involved in biogenesis of

235 small ribosomal subunits and were found to interact with the tomato mosaic virus (ToMV) movement protein
236 (MP) to promote virus movement [40,41].

237 The ZYMV virus manages to enter the cells through wounds or transported by aphids and moves from
238 cell to cell through the plasmodesms to reach the phloem where induce systemic infections. A delicate
239 equilibrium between RNA silencing and virus counter-defense responses in recovered leaves may help
240 maintain virus at levels below the threshold required for symptom induction. In TF, we found the up
241 regulation of a CYP82C2 (Cup000001g001147.1) that in Arabidopsis have a role in JA-induced defense-related
242 genes [42]. We also found exclusively expressed in TF two synaptotagmins (SYTA) that are key regulators of
243 plant virus intercellular movement, necessary for the ability of diverse cell-to-cell movement proteins and able
244 to regulate endocytosis and protein-mediated trafficking through plasmodesmata [43,44].

245 Genes involved in cytoskeleton organization, vesicular traffic and in callose deposition such as
246 Cup000021g019191.1 (LogFC 1.59) could affect the containment of the virus spread from cell to cell regulating
247 plasmodesmal permeability, resulted high activated in 381e [45,46]. By contrast, an upregulation of genes
248 involved in cell structure degradations (such as the pectin esterases) was observed in TF.

249 Comparing the two lines at genomic level, having nearby the same makeup, since 381e is a backcross line
250 derived from TF, we identify two regions in the tolerant line 381e enriched in SNPs. These regions could be
251 considered as introgressed from Menina and so putatively involved in the tolerance. The level of resistance of
252 381e to ZYMV is not as high as that of *C. moschata cv. Menina*, and some other gene could be involved in the
253 resistance regulation [6,47]. A marker located on chromosome 8, showing 90% co-segregation with resistance
254 in a F2 population derived from the cross between 381e and TF, was previously identified [11]. The correlation
255 of LG08SNP4 with resistance trait in F2 population (381e x TF) was also very high, supporting the finding of
256 Capuozzo et al., [11]. Whilst the lower correlation of LG01SNP1 with resistant phenotypes suggests that genes
257 with minor effects on the virus tolerance expression could be located there.

258 4. Conclusion

259 In conclusion, the network of expressed genes at 12 days after virus infection in 381e revealed recovery
260 of physiological processes, defense response activation, virus replication and movement limiting. Two
261 introgressed regions from Menina in 381e, contain NBS genes, serine/threonine and DEAD-box RNA helicases,
262 could be involved in tolerance to ZYMV. In particular, on linkage group eight might be located a major gene
263 responsible for tolerance and on linkage group one a minor gene with additive effect. Further efforts should
264 be performed to assess the contribution of different loci to ZYMV tolerance.

265 5. Materials and Methods

266 5.1 Plant material and ZYMV-inoculation

267

268 Two zucchini near-isogenic lines: TF (susceptible to ZYMV) and 381e (resistant to ZYMV) reported in
269 additional Figure 2, were used for RNA-seq experiment and DNA sequencing. The latter variety had been
270 derived from six generations of backcrossing to TF, selecting for resistance, followed by four successive
271 generations of self-pollination and selection for resistance [10]. Seeds of parental were sown in multi-cellular
272 trays consisting of 4 cm diameter pots that had been filled with peat, one per pot. After the seedlings were
273 transferred into pots 15 cm diameter and were grown under glasshouse condition at 22-24°C using supplement
274 lighting to maintain 12 hours photoperiod at the Research Centre for Plant Pathology (CRA-PAV) in Rome.
275 Each individual plant was assigned an identification number. An isolate of ZYMV from a naturally infected
276 plant of field-grown summer squash was used for experiments. The isolate causes the typical symptoms of
277 ZYMV disease including yellow mosaic, vein banding, blistering and malformation of leaves. Symptomatic
278 leaves of artificially infected zucchini plants were crushed, and the raw juice was extracted at a ratio 1:10 w/v
279 in 0.1 M phosphate buffer pH 7.2. Both cotyledons of test plants, sprinkled with the abrasive powder “celite”,
280 were inoculated with approximately 20 µl of the diluted extract, and subsequently washed with distilled
281 water. Finally, the DNA of a F2 segregating population (381e x TF) obtained by Capuozzo et al., was used for
282 molecular analysis [11].

283

284 5.2 Sample Collection and nucleic acid isolation

285

286 Twelve days after treatment, infected zucchini leaf samples of three independent replicates were
287 collected. Leaves were removed from the plants, weighed and immediately frozen in liquid nitrogen and
288 stored at -80°C . RNA was isolated using the RNeasy Plant Kit according to the manual instructions (Quiagen
289 Valencia, USA). RNA sample concentration was determined using a NanoDrop ND-1000 Spectrophotometer
290 (Nano-Drop Technologies, Wilmington, DE, USA) and by Bioanalyzer (Agilent Technologies). RNA integrity
291 was checked by horizontal electrophoresis on a 1.2% (w/v) agarose gel. Two μg of each sample were prepared
292 with 20 μl of 10 X RNA Loading Buffer composed by 400 μl Formamide, 10 μl 37% formaldehyde, 2 μl loading
293 buffer 10X (50% glycerol, 0.25% w/v bromophenol blue, 0.25% w/v xylene cyanol; Sigma) and 1 μl of 10 mg/ μl
294 SYBR Safe DNA Gel Stain (Invitrogen). Gel visualization was performed using UV light (UV Gel Doc
295 BIORAD). DNA was extracted from leaves of the 381e and TF not infected controls using DNeasy Plant Mini
296 Kit (Qiagen). DNA sample concentration was determined using a NanoDrop ND-1000 Spectrophotometer
297 (Nano-Drop Technologies, Wilmington, DE, USA).

298 In order to obtain high quantity of nucleic acid, total RNA from the six replicates was pooled in one
299 sample, obtaining three independent replicas for sequencing. Total purified RNA was converted to cDNA
300 libraries (QuantiTect Reverse Transcription Kit, Quiagen) and sequenced on Illumina HiSeq1500 platform at
301 the LabMedMolGe (Laboratory of Molecular Medicine and Genomics Department of Medicine and Surgery,
302 University of Salerno). The process generates millions (36 M) of short (100 bp) reads sequenced from both ends
303 of each cDNA fragment (paired-end sequencing).

304

305 5.3 RNA-Sequencing data analysis

306

307 The reads obtained from illumina sequencing, were analysed using the online platform A.I.R.
308 (<https://transcriptomics.sequentiabiotech.com>). FastQ files uploaded on A.I.R. platform were assessed by PCA
309 analysis both to recognize the file pairs and evaluate the quality of the samples. After the validation an

310 experimental label was provided, and the option pair-end sequences analysis was chosen. FastQ files of
311 inoculated and not inoculated condition for each sample were moved in the corresponding sections and
312 mapped against the *C. pepo* reference genome. Trimming of the reads, trimmed quality analysis, mapping,
313 BAM quality check and statistical analysis was provided by the platform. Clean FastQ files were analyzed by
314 DESeq2 algorithm to obtain DEGs. The DEGs list obtained from DESeq2 analysis, the PCA chart and other
315 general statistics data and lists, .bam and .bai files were downloaded. Genes having an FDR < 0.05 in DEGs
316 list was filtered to conduct further analyses. The *C.pepo* reference genome and relative gene annotation were
317 reported by Montero-Pau et al., (2017) and Andolfo et al., (2017) respectively [16,19]. Gene Ontology
318 Enrichment Analysis was performed using AgriGO version 2.0, REViGO was used to remove redundant GO
319 terms [48,49]. Genes were then considered significantly differentially expressed if the false discovery rate
320 (FDR) of the statistical test was less than 0.05.

321

322 5.4 Variant calling and genome plot construction

323

324 In order to detect small variants: SNPS and INDEL less than 50 base pairs on the transcripts of the susceptible
325 'TF' and resistant 381e accessions, a SNP calling analysis against the *Cucurbita pepo* reference genome was
326 performed. SNP calling, based on the two filtered .bam files, produced two VCF (Variant Call Format) files
327 (http://www.broadinstitute.org/igv/viewing_vcf_files) with the SNPs of each genotype in comparison to the
328 genome. To obtain the SNPs between both genotypes we found the common and unique SNPS between both
329 VCF files, removing at the same time SNPs at low quality/coverage and inconsistent SNPs. Finally, the circular
330 multi-track plot was carried out using the 'RCircos' R software package [50]. Vcf files were used to obtain .bed
331 files using bedtools, and *C. pepo* genome released by Montero-Pau et al. was used as reference [16].

332

333 5.5 Validation of predicted variants

334

335 A pool of 6 coding DNA regions was selected to perform molecular validation in 381e and TF.
336 PCR was executed with 25 ng of genomic or complementary DNA, 10 pmol primers, 1 U of Taq DNA
337 polymerase Kit (Invitrogen, Carlsbad, CA, USA), 10 pmol dNTPs, and 2 mM MgCl₂ in 25 µl reaction volumes.
338 Amplification was performed using the following cycling conditions: 1 min at 94 °C, followed by 30 cycles of
339 1 min at 94 °C, 1 min 30 s at 60 °C and 2 min at 72 °C, with a final extension for 7 min at 72 °C. Amplicons were
340 separated by electrophoresis on agarose gel (1.5 %), and photographed by a GelDoc apparatus. Primers were
341 designed with Primer3 (<http://frodo.wi.mit.edu>), with a length between 18 and 27 bp. The length of the
342 amplified fragments ranged from 300 to 1,000 bp, and the T_m of the specific primers was 59 °C for all pairs of
343 primers (Online Resource S4). Amplicons were sequenced using the BigDye Terminator Cycle Sequencing Kit
344 (Applied Biosystems, Foster City, CA, USA) and run on automated DNA sequencers (ABI PRISM 3100 DNA
345 Sequencer, Applied Biosystems). Sequence data deriving from *C. pepo* v4.1 reference genome were aligned
346 with corresponding sequences originated from amplicons using MUSCLE 3.6 [51].

347 **Additional Materials:** Additional Table 1: Number of short variants (SNV and InDel) identified in TF and 381e. Additional
348 Table 2: Number of short variants (SNV and InDel) identified in TF and 381e on LG01 and LG08. Additional Table 3:
349 Validation of 6 polymorphic loci located on putative genomic regions introgressed from Menina. (1): List of expressed
350 genes; (2): Differentially expressed genes (DEGs); (3): Gene ontology annotation (GO); (4): Up regulated genes, (5); Down
351 regulated genes. Additional Figure 1: Gel electrophoretic separation of digested PCR products. Additional Figure 2:
352 Comparison of the ZYMV tolerant line 381e (left) and the susceptible True French (right) 12 days after ZYMV inoculation

353 **Declarations**

354 **Data Availability:** The data set supporting the results of this article is available in the Sequence Read Archive (SRA)
355 repository of NCBI under the GEO accession number: GSE159530.

356 **Author Contributions:** Conceptualization, M.R.E.; methodology, G.A, C.C and A.D.D; validation, C.G.A; formal analysis,
357 C.G.A, G.A, C.C, A.D.D, C.M; investigation, L.T; resources Supervision GA and AD.D; M.R.E.; writing—original draft
358 preparation C.G.A, G.A and M.R.E; writing—review and editing, C.M and L.T; project funding acquisition, M.R.E. All
359 authors have read and agreed to the published version of the manuscript.

360 **Funding:** This research was funded by the Ministry of University and Research (GenHORT project).

361 **Acknowledgments:** We thank La Semiorto Sementi S.r.l. for plant material and Romanos Zois, Erasmus student from
362 Wageningen University (NL), for support in molecular analysis.

363 **Conflicts of Interest:** The authors declare no conflict of interest.

364 **Abbreviations**

ZYMV	Zucchini Yellow Mosaic Virus
DPI	Days Post Inoculation
DEGs	Differentially Expressed Genes
SYTA	Synaptotagmin
CNL	Coiled-Coil Nucleotide binding domain Leucine rich repeat
TF	True French
FDR	False Discovery Rate
GO	Gene Ontology
ROS	Reactive Oxygen Species
PEP	Phosphoenolpyruvate carboxylase
GAPDH	Glyceraldehyde 3-phosphate dehydrogenase
HSP	Heat Shock Protein
SNV	Single Nucleotide Variants
INDEL	Insertion and Deletion
LG	Linkage Group
NLR	Nucleotide binding Like Protein
PPR	Proteins and Receptor like Kinase
CDF	Coding DNA Fragments
NBS	Nucleotide Binding Site

365 **References**

- 366 1. Castle SJ, Perring TM, Farrar CA, Kishaba A. Field and laboratory transmission of watermelon mosaic virus 2 and
367 zucchini yellow mosaic virus by various aphid species. *Phytopatol.* 1992; 82: 235-240
- 368 2. Desbiez C, Lecoq H. Zucchini yellow mosaic virus. *Plant Path.* 1997; 46: 809-829. doi:10.1046/j.1365-3059.1997.d01-87.x
- 369 3. Katis NI, Tsitsipis JA, Lykouressis DP, Papapanayotou A, Margaritopoulos JT, Kokinis GM, Perdakis DC,
370 Manoussopoulos IN. Transmission of zucchini yellow mosaic virus by colonizing and non-colonizing aphids in
371 Greece and new aphid species vectors of the virus. *Journal of Phytopathology.* 2006; 154: 293–302.
- 372 4. Robinson RW, Weeden NF, Provvidenti R. Inheritance of resistance to zucchini yellow mosaic virus in the
373 interspecific cross *Cucurbita maxima* x *C. ecuadorensis*. *Cucurbit Genetics Cooperative Report.* 1988; 11: 74-75
- 374 5. Leibman D, Wolf D, Saharan V, Zelcer A, Arazi T, Yoel S, Gaba V, Gal-On A. A high level of transgenic viral small
375 RNA is associated with broad potyvirus resistance in cucurbits. *Mol. Plant–Microbe Interact.* 2011; 24: 1220–1238.
- 376 6. Pachner M, Paris H.S, Lelley T. Genes for resistance to zucchini yellow mosaic in tropical pumpkin. *J Hered.* 2011;
377 102: 330-335. doi:10.1093/jhered/esr006
- 378 7. Paris HS, Cohen S, Burger Y, Yoseph R. Singlegene resistance to zucchini yellow mosaic virus in *Cucurbita moschata*.
379 *Euphytica.* 1988; 37: 27-29.
- 380 8. Pachner M, Lelley T. Different genes for resistance to zucchini yellow mosaic virus (ZYMV) in *Cucurbita moschata*.
381 In: Lebeda A, Paris H.S, (eds) *Progress in cucurbit genetics and breeding research. Proc Cucurbitaceae.* 2004; 8th
382 EUCARPIA meeting on cucurbit genetics and breeding, Olomouc, 237–243
- 383 9. Nacar Ç, Fidan H, Ekbiç E, Aras V, Denli, N, Keles D. Development of suitable sources of resistance to ZYMV in
384 *Cucurbita pepo*. *Cucurbitaceae.* 2012; *Proceedings of the 10th EUCARPIA Meeting on Genetics and Breeding of*
385 *Cucurbitaceae, Antalya, Turkey, 15-18 October, 633-637*
- 386 10. Paris HS, Cohen S. Oligogenic inheritance for resistance to Zucchini yellow mosaic virus in *Cucurbita pepo*. *Annals*
387 *of Applied Biology.* 2000; 136: 209-214. doi:10.1111/j.1744-7348.2000.tb00027.x
- 388 11. Capuozzo C, Formisano G, Iovieno P, Andolfo G, Tomassoli L, Barbella MM, Pico B, Paris HS, Ercolano MR.
389 Inheritance analysis and identification of SNP markers associated with ZYMV resistance in *Cucurbita pepo*. *Mol*
390 *Breeding.* 2017; 37: 99. DOI 10.1007/s11032-017-0698-5
- 391 12. Pachner M, Paris HS, Winkler J, Lelley T. Phenotypic and marker-assisted pyramiding of genes for resistance to
392 zucchini yellow mosaic virus in oilseed pumpkin (*Cucurbita pepo*). *Plant Breed.* 2015; 134: 121-128.
393 doi:10.1111/pbr.12219

- 394 13. Anagnostou K, Jahn M, Perl-Treves R. Inheritance and linkage analysis of resistance to zucchini yellow mosaic virus,
395 watermelon mosaic virus, papaya ringspot virus and powdery mildew in melon. *Euphytica*. 2000; 116: 265–270.
396 doi.org/10.1023/A:1004005716806
- 397 14. Park Y, Katzir N, Brotman Y, King J, Bertrand F, Havey M. Comparative mapping of ZYMV resistances in cucumber
398 (*Cucumis sativus* L.) and melon (*Cucumis melo* L.). *Theor Appl Genet*. 2004; 109: 707–712. doi.org/10.1007/s00122-004-
399 1684-y
- 400 15. Iovieno P, Andolfo G, Schiavulli A, Catalano D, Ricciardi L, Frusciante L, Ercolano MR, Pavan S. Structure, evolution
401 and functional inference on the *Mildew Locus O* (*MLO*) gene family in three cultivated Cucurbitaceae *spp*. *BMC*
402 *Genomics*. 2015; 16: 1112. https://doi.org/10.1186/s12864-015-2325-3
- 403 16. Montero-Pau J, Blanca J, Bombarely A, Ziarsolo P, Esteras C, Martí-Gómez C, Ferriol M, Gómez P, Jamilena M,
404 Mueller L, Picó B, Cañizares J. De novo assembly of the zucchini genome reveals a whole-genome duplication
405 associated with the origin of the *Cucurbita* genus. *Plant Biotechnol J*. 2018; 16: 1161-1171. doi:10.1111/pbi.12860
- 406 17. Wyatt L, Strickler S, Mueller L, Mazourek M. An acorn squash (*Cucurbita pepo* ssp. *ovifera*) fruit and seed
407 transcriptome as a resource for the study of fruit traits in *Cucurbita*. *Hortic Res*. 2015; 2:14070.
408 https://doi.org/10.1038/hortres.2014.70
- 409 18. Xanthopoulou A, Psomopoulos F, Ganopoulos I, Manioudaki M, Tsaftaris A, Nianiou-Obeidat I, Panagiotis M. De
410 novo transcriptome assembly of two contrasting pumpkin cultivars. *Genomics Data*. 2016; 7: 200–201.
411 https://doi.org/10.1016/j.gdata.2016.01.006.
- 412 19. Andolfo G, Di Donato A, Darrudi R, Errico A, Aiese Cigliano R, Ercolano MR. Draft of Zucchini (*Cucurbita pepo* L.)
413 Proteome: A Resource for Genetic and Genomic Studies. *Front Genet*. 2017; 8: 181
- 414 20. Inoue H, Li M, Schnell DJ. An essential role for chloroplast heat shock protein 90 (Hsp90C) in protein import into
415 chloroplasts. *Proc Natl Acad Sci U S A*. 2013; 110: 3173-3178. doi:10.1073/pnas.1219229110
- 416 21. Rajniak J, Barco B, Clay N, Sattely E. A new cyanogenic metabolite in *Arabidopsis* required for inducible pathogen
417 defence. *Nat*. 2015; 525: 376–379. doi.org/10.1038/nature14907
- 418 22. Zellnig G, Pöckl MH, Möstl S, Zechmann B. Two- and three-dimensional characterization of Zucchini Yellow Mosaic
419 Virus induced structural alterations in *Cucurbita pepo* L. plants. *J Struct Biol*. 2014; 186: 245–252.
- 420 23. Bengyella L, Waikhom SD, Allie F, Rey C. Virus tolerance and recovery from viral induced symptoms in plants are
421 associated with transcriptome reprogramming. *Plant Mol Biol*. 2015; 89: 243-252. doi:10.1007/s11103-015-0362-6

- 422 24. Hanley-Bowdoin L, Bejarano E, Robertson D, Mansoor S. Geminiviruses: masters at redirecting and reprogramming
423 plant processes. *Nat Rev Microbiol.* 2013; *11*: 777–788. doi.org/10.1038/nrmicro3117
- 424 25. Ghoshal B, Sanfaçon H. Symptom recovery in virus-infected plants: Revisiting the role of RNA silencing mechanisms.
425 *Virology.* 2015; 479-480: 167-179. doi.org/10.1016/j.virol.2015.01.008.
- 426 26. Nigam D, LaTourrette K, Souza Pedro FN, Garcia-Ruiz H. Genome-Wide Variation in Potyviruses. *Front in Plant Sci.*
427 2019; *10*: 1439. doi=10.3389/fpls.2019.01439
- 428 27. Wu CY, Nagy PD. Blocking tombusvirus replication through the antiviral functions of DDX17-like RH30 DEAD- box
429 helicase. *PLoS Pathog.* 2019; *15*:128. doi.org/10.1371/journal.ppat.1007771
- 430 28. Pandey S, Prasad A, Sharma N, Prasad M. Linking the plant stress responses with RNA helicases. *Plant Sci.* 2020;
431 299. doi.org/10.1016/j.plantsci.2020.110607.
- 432 29. Kumar S, Karmakar R, Gupta I, Patel AK. Interaction of potyvirus helper component-proteinase (HcPro) with
433 RuBisCO and nucleosome in viral infections of plants. *Plant Physiol Biochem.* 2020; *151*: 313–322
- 434 30. Nováková S, Flores-Ramírez G, Glasa M, Danchenko M, Fiala R, Skultety L. Partially resistant Cucurbita pepo
435 showed late onset of the Zucchini yellow mosaic virus infection due to rapid activation of defense mechanisms as
436 compared to susceptible cultivar. *Front Plant Sci.* 2015; *6*: 263. doi:10.3389/fpls.2015.00263
- 437 31. Oh SE, Yeung C, Babaei-Rad R, Zhao R. Cosuppression of the chloroplast localized molecular chaperone HSP90.5
438 impairs plant development and chloroplast biogenesis in Arabidopsis. *BMC Res Notes.* 2014; *7*:643
439 doi.org/10.1186/1756-0500-7-643
- 440 32. Hubert DA, Tornero P, Belkhadir Y, Krishna P, Takahashi A, Shirasu K, Dangl JL. Cytosolic HSP90 associates with
441 and modulates the *Arabidopsis* RPM1 disease resistance protein. *The EMBO Journal.* 2003; *22*: 5679-5689.
442 doi:10.1093/emboj/cdg547
- 443 33. Liu Y, Burch-Smith T, Schiff M, Feng S, Dinesh-Kumar SP. Molecular chaperone Hsp90 associates with resistance
444 protein N and its signalling proteins SGT1 and Rar1 to modulate an innate immune response in plants. *J Biol Chem.*
445 2004; *279*: 2101-2108. doi:10.1074/jbc.M310029200
- 446 34. Aoki K, Kragler F, Xoconostle-Cazares B, Lucas WJ. A subclass of plant heat shock cognate 70 chaperones carries a
447 motif that facilitates trafficking through plasmodesmata. *Proc Natl Acad Sci U S A.* 2002; *99*: 16342-16347. doi:
448 10.1073/pnas.252427999.
- 449 35. Zhang XP, Glaser E. Interaction of plant mitochondrial and chloroplast signal peptides with the Hsp70 molecular
450 chaperone, *Trends Plant Sci.* 2002; *7*: 14–21.

- 451 36. Osuna-Cruz CM, Paytuví-Gallart A, Di Donato A, Sundesha V, Andolfo G, Aiese Cigliano R, Sanseverino W,
452 Ercolano MR. PRGdb 3.0: a comprehensive platform for prediction and analysis of plant disease resistance
453 genes, *Nucleic Acids Research*. 2018; 46: 1197–1201. doi.org/10.1093/nar/gkx1119
- 454 37. Niehl A, Wyrsh I, Boller T, Heinlein M. Double-stranded RNAs induce a pattern-triggered immune signaling
455 pathway in plants. *New Phytol*. 2016; 211: 1008-1019. doi:10.1111/nph.13944
- 456 38. Andolfo G, Jupe F, Witek K, Etherington G, Ercolano MR, Jones JDG. Defining the full tomato NB-LRR resistance
457 gene repertoire using genomic and cDNA RenSeq. *BMC Plant Biol*. 2014; 14: 120. doi.org/10.1186/1471-2229-14-120
- 458 39. Andolfo G, Di Donato A, Chiaiese P, De Natale A, Pollio A, Jones JDG, Frusciante L, Ercolano MR. Alien Domains
459 Shaped the Modular Structure of Plant NLR Proteins. *Genome Biology and Evolution*. 2019; 11: 3466–
460 3477. doi.org/10.1093/gbe/evz248
- 461 40. Gao Q, Xu S, Zhu X, Wang L, Yang Z, Zhao X. Genome-wide identification and characterization of the RIO atypical
462 kinase family in plants. *Genes Genom*. 2018; 40: 669–683. doi.org/10.1007/s13258-018-0658-4
- 463 41. Yoshioka K, Matsushita Y, Kasahara M, Konagaya K, Nyunoya H. Interaction of tomato mosaic virus movement
464 protein with tobacco RIO kinase. *Mol Cells*. 2004; 17:223–229
- 465 42. Uchiyama A, Shimada-Beltran H, Levy A, Zheng JY, Javia PA, Lazarowitz SG. The Arabidopsis synaptotagmin
466 SYTA regulates the cell-to-cell movement of diverse plant viruses, *Front in Plant Sci*. 2014; 5: 584
- 467 43. Lewis DJ, Lazarowitz SG. Arabidopsis synaptotagmin SYTA regulates endocytosis and virus movement protein cell-
468 to-cell transport. *Proceedings of the National Academy of Sciences*. 2010; 107: 2491-
469 2496. doi:10.1073/pnas.0909080107
- 470 44. Li W, Zhao Y, Liu C, Yao G, Wu S, Hou C, Zhang M, Wang D. Callose deposition at plasmodesmata is a critical factor
471 in restricting the cell-to-cell movement of *Soybean mosaic virus*. *Plant Cell Rep*. 2012; 31: 905–916.
472 doi.org/10.1007/s00299-011-1211-y
- 473 45. Bo X, Yunfei D, Masahiro M, Kanaoka KO, Zonglie H. Expression of Arabidopsis callose synthase 5 results in callose
474 accumulation and cell wall permeability alteration. *Plant Sci*. 2012; 183: 1-8. doi.org/10.1016/j.plantsci.2011.10.015
- 475 46. Liu F, Jiang H, Ye S, Chen W, Liang W, Xu Y, Sun B, Sun J, Wang Q, Cohen JD, Li C. The Arabidopsis P450 protein
476 CYP82C2 modulates jasmonate-induced root growth inhibition, defense gene expression and indole glucosinolate
477 biosynthesis. *Cell Res*. 2010; 20: 539–552. doi.org/10.1038/cr.2010.36
- 478 47. Paris HS, Brown R. The Genes of Pumpkin and Squash. *HortSci*. 2005; 40: 1620-1630.

- 479 48. Tian T, Yue L, Hengyu Y, Qi Y, Xin Y, Zhou D, Wenying X, Zhen S. agriGO v2.0: a GO analysis toolkit for the
480 agricultural community, 2017 update. *Nucleic Acids Res.* 2017; gkx382. doi: 10.1093/nar/gkx382
- 481 49. Supek F, Bošnjak M, Škunca N, Šmuc T. REVIGO Summarizes and Visualizes Long Lists of Gene Ontology Terms.
482 *PLoS ONE.* 2011; 6. doi.org/10.1371/journal.pone.0021800
- 483 50. Zhang H, Meltzer P, Davis S. RCircos: an R package for Circos 2D track plots. *BMC Bioinformatics.* 2013; 14: 244.
484 doi.org/10.1186/1471-2105-14-244
- 485 51. Edgar RC. MUSCLE: multiple sequence alignment with high accuracy and high throughput, *Nucleic Acid Research.*
486 2004; 32: 1792-97.

Figures

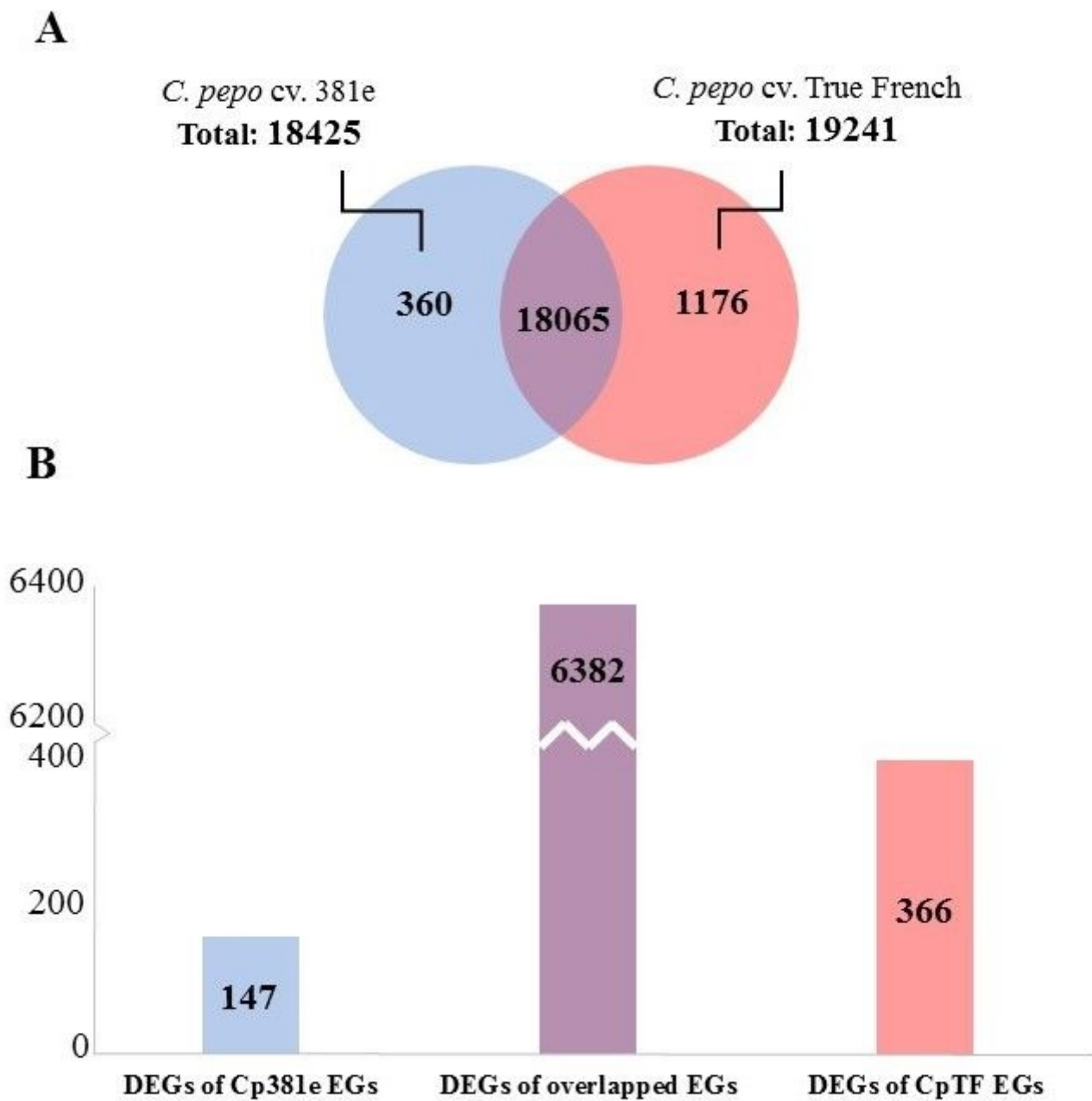


Figure 1

Transcriptional Profile. A) Total Expressed Genes in *C. pepo* 381e (blue), TF (orange), and overlapped genes (violet). B) Differentially Expressed Genes for each area of Venn diagram. 2.2 Overview of cellular processes activated in the tolerant and susceptible line

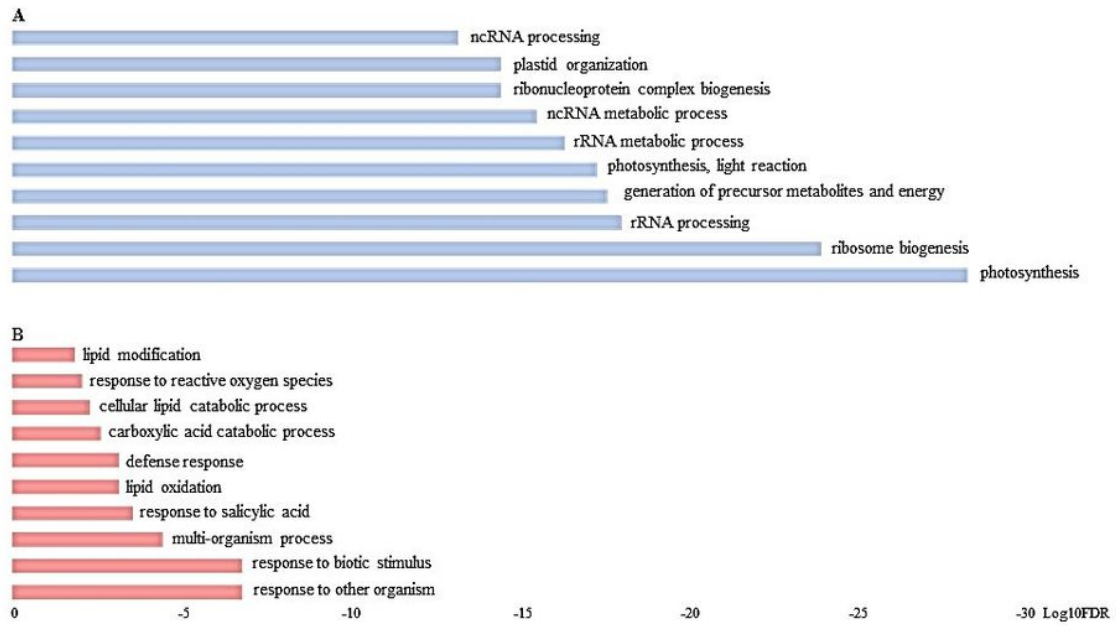


Figure 2

Top ten of non-redundant significantly enriched GO terms in biological process category. A) Upregulated genes in 381e and B) Upregulated genes in True French. The categories size is related to LOG₁₀ FDR of enriched GOs.

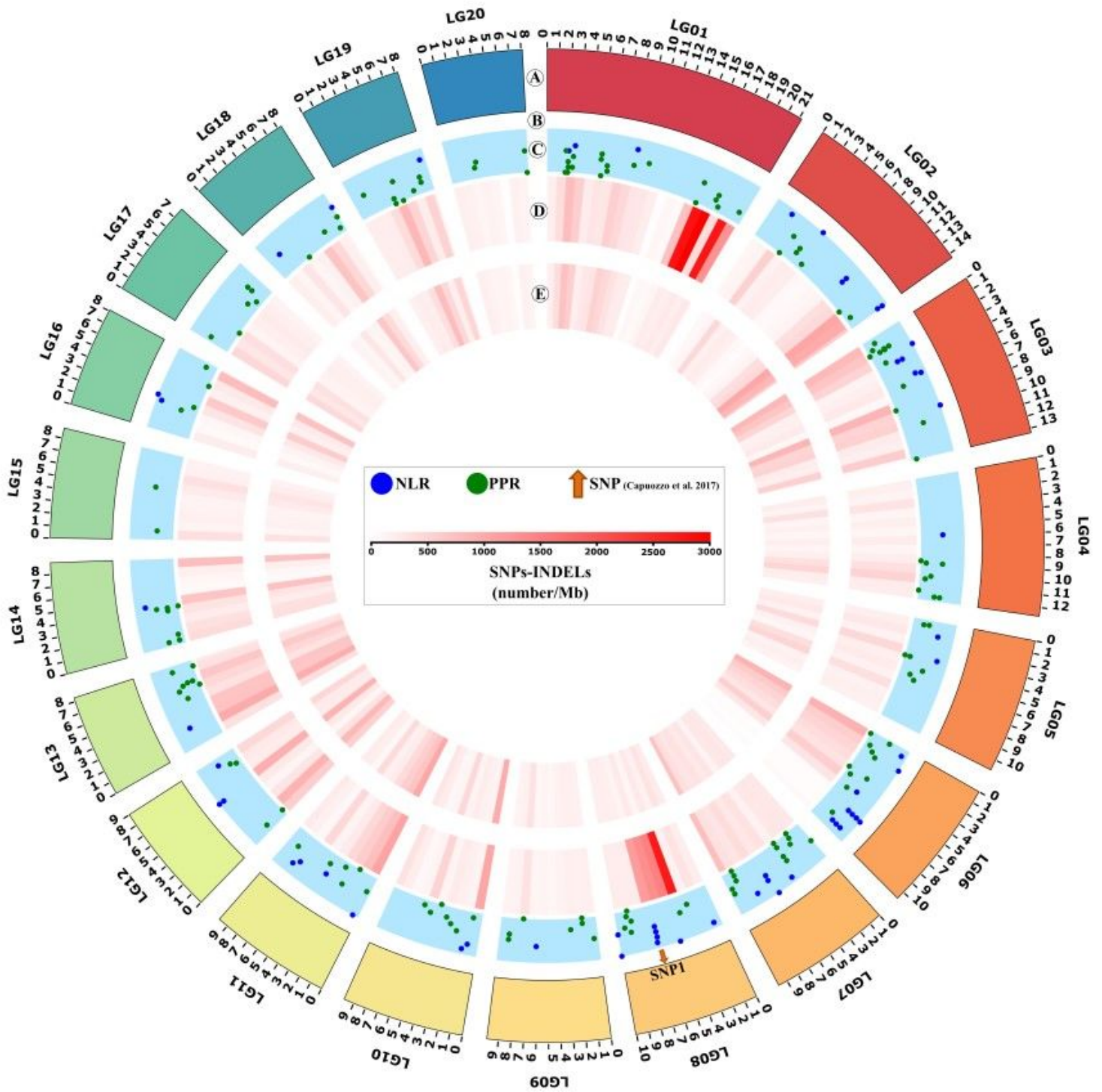


Figure 3

Circos plot integrating the genomic positions of ZYMV-related markers, pathogen recognition genes and small variants (SNP: single nucleotide polymorphisms and InDel: insertion and deletion). Inset legend providing information represented by each data ring. Track A denotes the 20 pseudo-chromosomes (LG: linkage group) of *Cucurbita pepo*. The length of each circle segment represents the size of pseudo-chromosomes expressed in megabases (Mb). B) The marker associated to ZYMV tolerance identified by Capuozzo et al. [11] is indicated by orange arrow. C) Genomic positions of nucleotide

binding like proteins (NLR; blue spots) and receptor like proteins and receptor like kinase (PPR; green spots), annotated by Andolfo et al. [19], are shown as scatterplots. Heatmaps for the density levels (number/Mb) of small variants identified in (D) *C. pepo* 381e and (E) *C. pepo* TF cultivars.

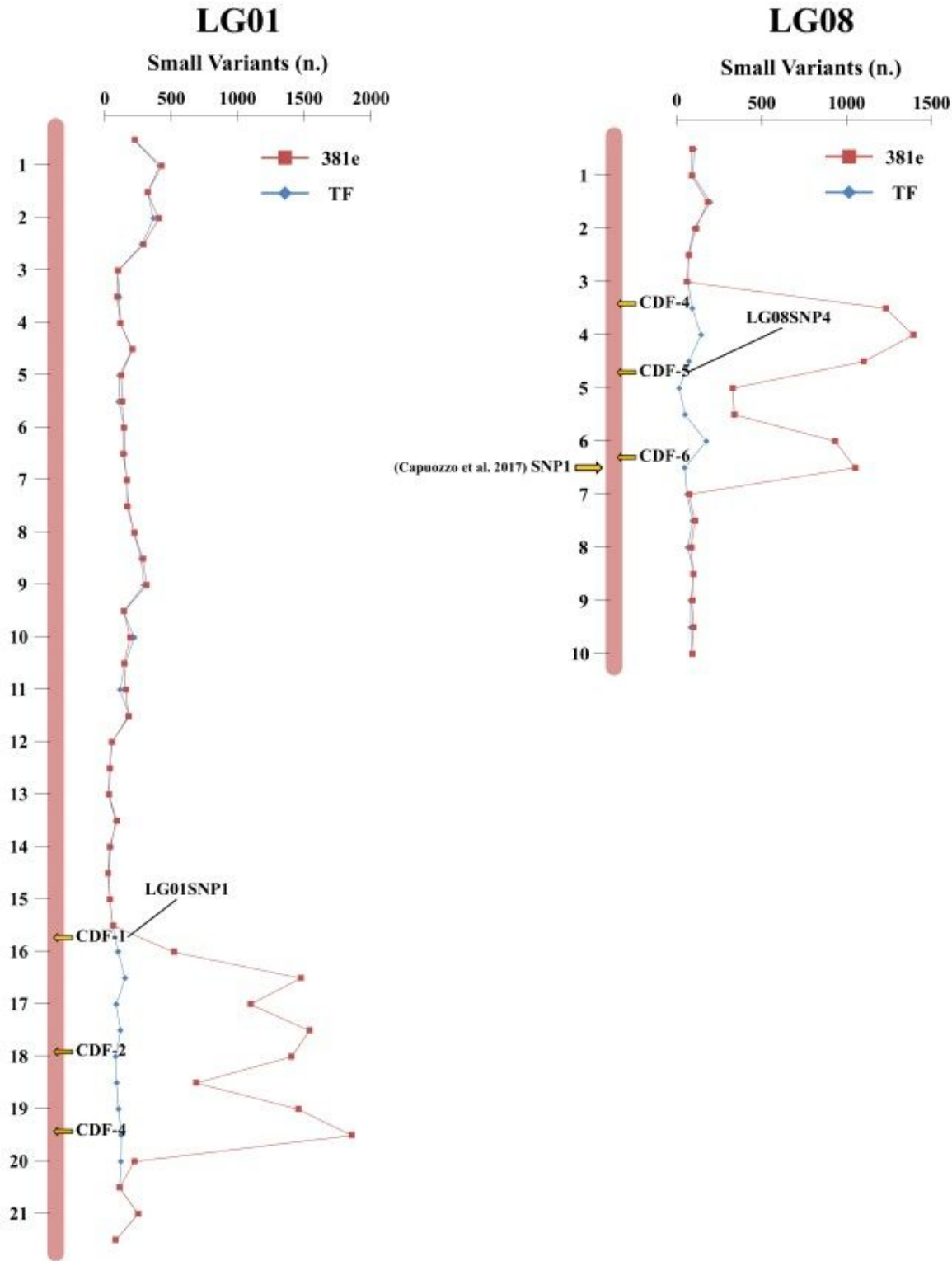


Figure 4

High resolution map integrating genomic and genetic marker information. The distribution of small variants along 1 and 8 pseudochromosomes was reported (381e in red and TF in blue). The genomic

position of six coding DNA fragments (CDFs) and two CAPS markers (LG01SNP1 and LG08SNP4) was indicated.

Supplementary Files

This is a list of supplementary files associated with this preprint. Click to download.

- [Supplementarymaterials.xlsx](#)